Amino Acids
DOI 10.1007/s00726-016-2263-7

ORIGINAL ARTICLE

Inhibition of tyrosine phenol-lyase by tyrosine homologues

Quang Do[1,3] · Giang T. Nguyen[1,4] · Robert S. Phillips[1,2]

Received: 26 December 2015 / Accepted: 20 May 2016

Abstract We have designed, synthesized, and evaluated tyrosine homologues and their *O*-methyl derivatives as potential inhibitors for tyrosine phenol lyase (TPL, E.C. 4.1.99.2). Recently, we reported that homologues of tryptophan are potent inhibitors of tryptophan indole-lyase (tryptophanase, TIL, E.C. 4.1.99.1), with K_i values in the low μM range (Do et al. Arch Biochem Biophys 560:20–26, 2014). As the structure and mechanism for TPL is very similar to that of TIL, we postulated that tyrosine homologues could also be potent inhibitors of TPL. However, we have found that homotyrosine, bishomotyrosine, and their corresponding *O*-methyl derivatives are competitive inhibitors of TPL, which exhibit K_i values in the range of 0.8–1.5 mM. Thus, these compounds are not potent inhibitors, but instead bind with affinities similar to common amino acids, such as phenylalanine or methionine. Pre-steady-state kinetic data were very similar for all compounds tested and demonstrated the formation of an equilibrating mixture of aldimine and quinonoid intermediates upon binding. Interestingly, we also observed a blue-shift for the absorbance peak of external aldimine complexes of all tyrosine homologues, suggesting possible strain at the active site due to accommodating the elongated side chains.

Keywords Pyridoxal-5′-phosphate · Reaction mechanism · β-Elimination · Stopped-flow kinetics · Amino acid homologue

Abbreviations

PLP	Pyridoxal-5′-phosphate
TPL	Tyrosine phenol-lyase [EC 4.1.99.2]
TIL	Tryptophan indole-lyase [EC 4.1.99.1]
SOPC	S-(*o*-Nitrophenyl)-L-cysteine

Introduction

Tyrosine phenol-lyase (TPL, [E.C. 4.1.99.2]) is a pyridoxal-5′-phosphate (PLP)-dependent bacterial enzyme that catalyzes the reversible hydrolytic cleavage of the C_β–C_γ bond of L-Tyr to phenol and ammonium pyruvate (Eq. 1) (Yamada et al. 1968; Kumagai et al. 1970a, b). In addition to its physiological substrate, TPL also catalyzes the in vitro β-elimination of substrates with good leaving groups on the β-carbon, including L-serine, L-cysteine, S-(*o*-nitrophenyl)-L-cysteine (SOPC) (Eq. 2), *O*-acetyl-L-serines, and S-alkyl-L-cysteines (Eq. 3) (Yamada et al. 1968; Kumagai et al. 1970a; Phillips 1987). As the cleavage of L-Tyr is reversible, TPL was also utilized in the enzymatic production of L-Tyr (Phillips et al. 1989) and β-substitution reactions in the synthesis of 3,4-dihydroxyphenyl-L-alanine (L-dopa) (Kumagai et al. 1969), and aza-L-tyrosine (Watkins and Phillips 2001).

Handling Editor: C. Schiene-Fischer.

Electronic supplementary material The online version of this article (doi:10.1007/s00726-016-2263-7) contains supplementary material, which is available to authorized users.

✉ Robert S. Phillips
plp@uga.edu

[1] Department of Chemistry, University of Georgia, Athens, GA 30602, USA

[2] Department of Biochemistry and Molecular Biology, University of Georgia, Athens, GA 30602, USA

[3] Present Address: Hill Manufacturing Co., Inc., 1500 Jonesboro Rd SE, Atlanta, GA 30315, USA

[4] Present Address: Adelaide, Australia

Published online: 26 May 2016

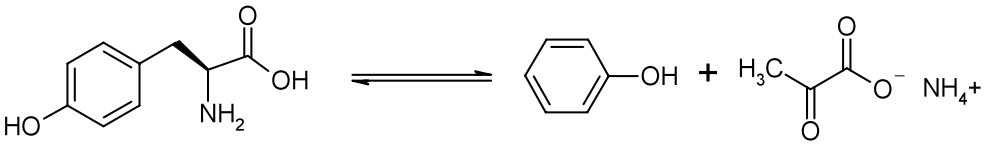

(1)

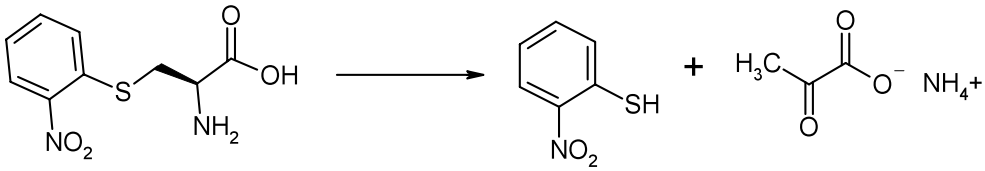

(2)

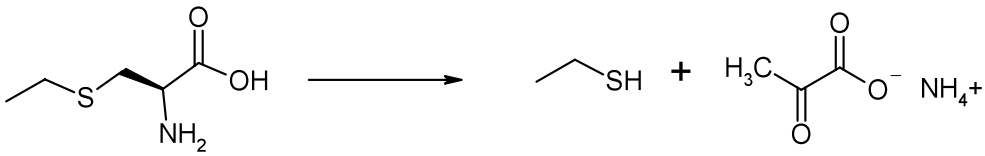

(3)

The postulated mechanism of TPL consists of several steps, in which formation of a quinonoid carbanionic intermediate is an essential step of the catalytic cycle (Scheme 1) (Muro et al. 1978; Phillips et al. 2002, 2006; Milić et al. 2011). The first step is transaldimination, in which the internal aldimine is transformed into an external aldimine upon binding of the substrate. Subsequent deprotonation of the C_α proton, by the amino side chain of Lys257, gives rise to the quinonoid intermediate. Ketonization of the phenol, accompanied by C_γ protonation, subsequently leads to the cleavage of the C_β–C_γ bond to form free phenol and an aminoacrylate intermediate. Previously, we and others studied kinetics and structures of quinonoid complexes and provided further evidence for a quinonoid structure as the key intermediate in the TPL mechanism (Muro et al. 1978; Phillips et al. 2002, 2006;

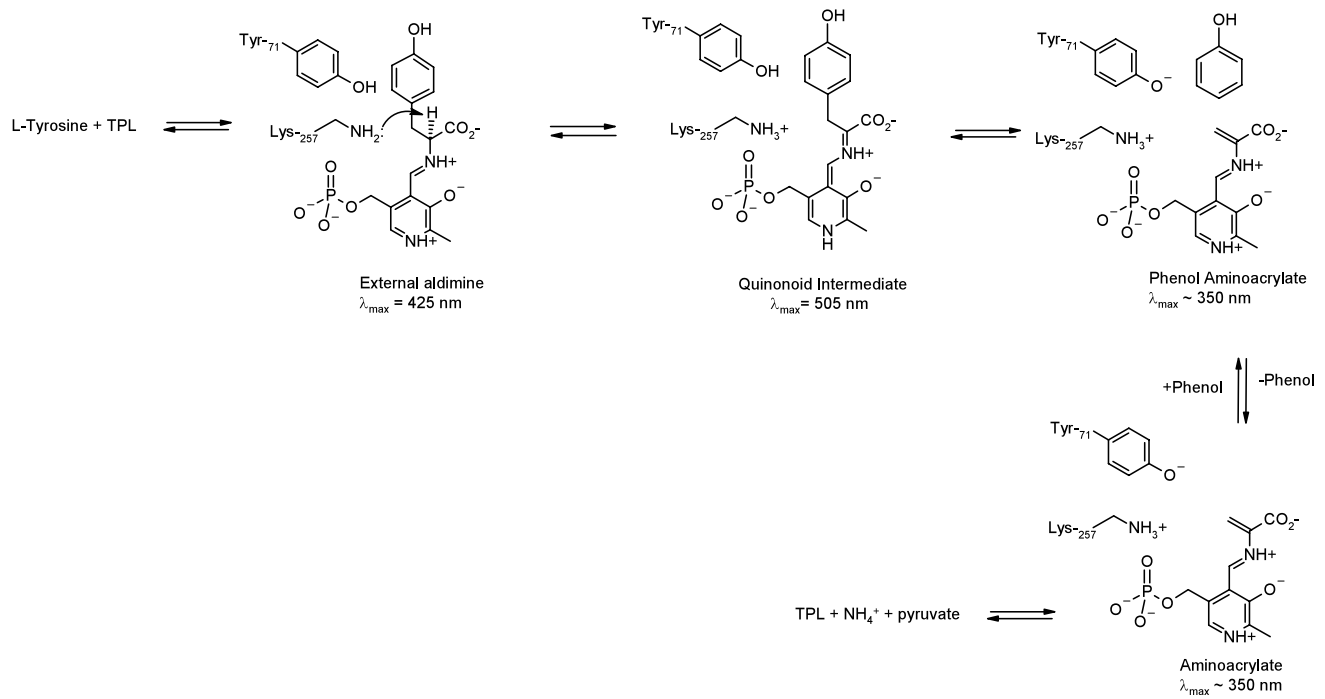

Scheme 1 Proposed β-elimination mechanism of TPL

Milić et al. 2008, 2011). Furthermore, the crystal structure of F448H TPL with a bound substrate shows evidence for a contribution of ground state strain to catalysis, since a closed conformation of the quinonoid intermediate shows the substrate aromatic ring bent ~20° out of plane (Milić et al. 2011). However, it remains unclear if C_γ proton transfer and C_β–Cγ cleavage follow a stepwise or concerted mechanism.

Tryptophan indole-lyase (tryptophanase, TIL, E.C. 4.1.99.1) is another PLP-dependent bacterial enzyme that catalyzes the analogous reversible (Watanabe and Snell 1972) hydrolytic cleavage of the C_β–C_γ bond of tryptophan to indole and ammonium pyruvate (Snell 1975). TPL and TIL from various bacteria share about 40 % sequence identity, and both enzymes adopt virtually identical three-dimensional folds (Antson et al. 1993; Isupov et al. 1998). Also, the accepted mechanism for TIL (Phillips 1991, 2000; Do et al. 2014) is remarkably similar to that suggested for TPL in the cleavage of their respective substrates. However, the two enzymes show strict specificity for their physiological substrates. Recently, we reported the evaluation of mechanism-based inhibitors for TIL and discovered that homologation of the physiological substrate, L-tryptophan, resulted in potent inhibitors of TIL (Do et al. 2014). Our rationale was to design a transition-state analog inhibitor resembling the elongated transition-state structure of the indolenine intermediate, or a bi-product analog of the phenol-aminoacrylate complex immediately after bond cleavage. Since TIL and TPL have similar structures and mechanisms, and with the encouraging results from our previous work, we were interested in extending our design and rationale to search for new mechanism-based inhibitors of TPL. Inhbitors of TIL have played a role in the determination of the physiological effects of the indole product (Di Martino et al. 2002; Venkatesh et al. 2014), and the availability of comparable potent TPL inhibitors may assist in elucidation of the hitherto unknown physiological function of the phenol produced by TPL.

In the present work, we postulated that inhibitors that structurally resemble the elongated transition-state structure leading from the proposed keto-quinonoid intermediate to the product complex can potentially inhibit TPL. Based on that rationale, we proposed that homologues of the physiological substrate, L-tyrosine, may inhibit TPL activity. This work describes the synthesis, steady-state, and pre-steady-state kinetic evaluations of L-homotyrosine (**1a**) and L-bishomotyrosine (**1b**) as possible mechanism-based inhibitors for TPL (Fig. 1). The quinonoid intermediate was also proposed to form a closed conformation in which hydrogen bonding from the hydroxyl group contributes to the C_α–C_β–C_γ angle strain to assist in the cleavage of the C_β–C_γ bond (Milić et al. 2011). Hence, we also evaluated methylated derivatives of tyrosine homologues,

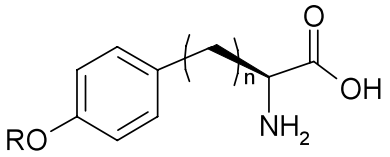

n=1, R=H, L-Tyrosine
n=2, R=H, **1a**; R=CH_3, **6a**
n=3, R=H, **1b**; R=CH_3, **6b**

Fig. 1 Structures of L-tyrosine and L-tyrosine homologues and derivatives

O-methyl-L-homotyrosine (**6a**) and *O*-methyl-L-bishomotyrosine (**6b**), as it would be of interest to explore whether methylation of the phenol OH would have an effect on the efficiency of the proposed compounds as inhibitors for TPL.

Materials and methods

Materials: Methylene chloride and ethanol were previously dried over CaH_2 and Mg, respectively, prior to use. 2-(4-Methoxyphenyl)ethanol (Acros), 3-(4-methoxyphenyl)propan-1-ol (Aldrich), triphenylphosphine (Aldrich), carbon tetrabromide (Janssen Chimica), diethyl acetamidomalonate (Aldrich), Aspergillus acylase I (0.43 unit/mg, Aldrich), pyridoxal-5′-phosphate (PLP) (USB Corp.), and all other reagents (Thermo Fisher Scientific) were used without further purification. S-(*o*-Nitrophenyl)-L-cysteine (SOPC) used in enzyme assays was prepared as previously described (Phillips et al. 1989). Enzyme assays were performed using distilled deionized water. All NMR data were collected on a 400-MHz Varian Mercury Plus NMR instrument, and data were processed by Mestrec MNova NMR processing software. ESI–MS experiments were performed on a Perkin Elmer Sciex API I Plus.

Synthesis of L-homotyrosine, L-bishomotyrosine, and *O*-methyl derivatives

*1-(2-Bromoethyl)-4-methoxybenzene (**3a**):* In a three-neck flask, 2-(4-methoxyphenyl)ethanol (**2a**, 3.00 g, 1 eq.) and triphenylphosphine (6.72 g, 1.3 eq.) were dissolved in dry CH_2Cl_2 (25 ml). In an addition funnel, carbon tetrabromide (8.50 g, 1.3 eq.) was dissolved in dry CH_2Cl_2 (15 ml) and added dropwise under inert atmosphere at 0 °C until the addition was complete. The reaction was allowed to stir at room temperature for an additional 4 h, or until complete disappearance of starting materials from thin-layer chromatography (TLC). The solvent was removed under reduced pressure, and the residue was purified by column

chromatography using hexane and EtOAc to yield **3a** as a clear oil. Yield: 4.11 g (97 %). 1H NMR ($CDCl_3$) δ (ppm): 3.08–3.12 (t, 2H), 3.51–3.55 (t, 2H), 3.79 (s, 3H), 6.85–6.87 (d, 2H), 7.12–7.14 (d, 2H).

*Diethyl 2-acetamido-2-(4-methoxyphenylethyl)malonate (**4a**):* In a three-neck flask, diethyl acetamidomalonate (5.25 g, 1.3 eq.) was added to a solution of dry ethanol (40 ml) containing dissolved sodium metal (0.556 g, 1.3 eq.) at 0 °C. The mixture was stirred for an additional 30 min at 0 °C. Then, compound **3a** (4.00 g, 1 eq.) was added in, and the solution was allowed to reflux under inert atmosphere for an additional 15 h. The solvent was removed under reduced pressure, and the residue was purified by column chromatography using hexane and EtOAc. Subsequent removal of the eluting solvent under reduced pressure yielded compound **4a**. Yield: 3.30 g (51 %).1H NMR ($CDCl_3$) δ (ppm): 1.23–1.27 (t, 6H), 2.00 (s, 3H), 2.40–2.43 (m, 2H), 2.64–2.68 (m, 2H), 3.78 (s, 3H), 4.19–4.22 (m, 4H), 6.77 (s, 1H), 6.80–6.82 (d, 2H), 7.05–7.07 (d, 2H).

*2-Acetamido-4-(4-methoxyphenyl)butanoic acid (**5a**):* In a round-bottom flask, NaOH (0.717 g, 2 eq.) was dissolved in aqueous tetrahydrofuran (1:1, THF:H_2O, 40 ml) solution, then compound **4a** (3.15 g, 1 eq.) was added, and the solution was allowed to reflux for 15 h. The solvent was then removed under reduced pressure, and the resulting residue was taken up in water and EtOAc. The aqueous layer was acidified to pH 2 using 6-M HCl and extracted with EtOAc. The organic layer was washed with water and dried over $MgSO_4$. Removal of the solvent under reduced pressure gave **5a** as a white solid. Yield: 2.17 g (96 %). 1H NMR (DMSO) δ (ppm): 1.94 (s, 3H), 3.78 (s, 3H), 4.12–4.15 (m, 1H), 6.90–6.92 (d, 2H), 7.15–7.17 (d, 2H), 8.25–8.27 (d, 1H), 12.5 (b, 1H).

*O-Methyl-L-homotyrosine (**6a**):* In an Erlenmeyer flask, compound **5a** (2.00 g) was dissolved in potassium phosphate buffer (80 ml, 100 mM), and the final pH was adjusted to 8 using 6-M NaOH. Then, Aspergillus acylase I (200 mg) was added to the mixture, and it was allowed to incubate overnight at 37 °C, with a shaking speed of 250 rpm (C25, New Brunswick Scientific). The resulting mixture was cooled, filtered, and washed with cold water to give pure **6a** as a crystalline solid. Yield: 573 mg (69 %). 1H NMR (D_2O/NaOD) δ (ppm): 1.61–1.70 (m, 2H), 2.38–2.42 (t, 2H), 3.03–3.06 (t, 1H), 3.62 (s, 3H), 6.76–6.78 (d, 2H), 7.05–7.07 (d, 2H).

*L-Homotyrosine (**1a**):* In a round-bottom flask, compound **6a** (0.1 g) was dissolved in concentrated HI. The mixture was allowed to reflux overnight, and HI was removed under reduced pressure. The residue was neutralized using phosphate buffer (pH 7). The solvent was removed under reduced pressure and a minimal amount of cold water was added to the residue. The mixture was cooled, filtered, and washed with water to give **1a** as a white solid. Yield: 68 mg (73 %). 1H NMR (D_2O/NaOD) δ (ppm): 1.54–1.62 (m, 2H), 2.24–2.28 (t, 2H), 3.04 (s, 1H), 6.34–6.36 (d, 2H), 6.79–6.81 (d, 2H).

*O-Methyl-L-bishomotyrosine (**6b**) and L-bishomotyrosine (**1b**):* Compounds **6b** and **1b** were obtained following the same procedure described above for **6a** and **1a**. Bromination of **2b** using Appel's salt afforded **3b** as a clear liquid in excellent yield (92 %). Subsequent alkylation using DEAM provided **4b** as a white solid (52 %). Ester hydrolysis and decarboxylation of **4b** was achieved in one step by refluxing in aqueous NaOH to yield **5b** as a white solid in excellent yield (92 %). Enantioselective hydrolysis of N-acetyl using Aspergillus acylase, as described above, provided **6b** in good yield (67 %). Deprotection using HI gave compound **1b** as a crystalline solid (69 % yield).

Enzymes and enzyme assays. Citrobacter freundii TPL was obtained from *Escherichia coli* SVS370/pTZTPL (Antson et al. 1993) and purified as previously described (Chen et al. 1995a). The purified enzyme was stored as aliquots at −78 °C and thawed immediately prior to use. Enzyme assays were performed on a Cary 1 UV–visible spectrophotometer equipped with a thermoelectric Peltier-controlled 6 × 6 cell changer. Enzyme activity was routinely determined using SOPC as previously described (Chen et al. 1995b), by following the absorbance decrease at λ = 370 nm ($\Delta\varepsilon = 1.86\ mM^{-1}\ cm^{-1}$). SOPC was used as the substrate in inhibition assays for TPL. All assays were conducted at 25 °C and in a total volume of 600 µl. A typical assay contained potassium phosphate buffer, pH 8.0 (50 mM), PLP (40 µM), and varying concentration of SOPC and inhibitors. Experimental velocities were analyzed, and K_i values were fit to Eq. 4 by the FORTRAN program, COMPO, of Cleland (1979). Enzyme concentration was estimated from the absorbance at λ = 278 nm ($A_{1\%} = 8.37$) (Kumagai et al. 1970a) assuming a subunit mass of 51 kDa (Antson et al. 1993).

$$v = V_{max} * [S]/((K_m(1 + [I]/K_i) + [S]) \quad (4)$$

Rapid-scanning stopped-flow experiments Rapid-scanning stopped-flow experiments were performed on an RSM-1000 spectrophotometer (OLIS, Inc), equipped with a stopped-flow cell of 1-cm pathlength, capable of collecting up to 1000 scans per second with a dead time of ~2 ms. Prior to performing kinetic experiments, the enzyme was incubated with 0.5-mM PLP for 30 min at 30 °C. Subsequently, the enzyme was eluted through a short gel filtration column (PD-10, GE Healthcare) equilibrated with phosphate buffer (pH 8.0, 50 mM) to remove excess PLP, and rapid-scanning experiments were carried out in the same buffer. The final concentration of the ligand was 5 mM. Rapid-scanning stopped-flow data were processed

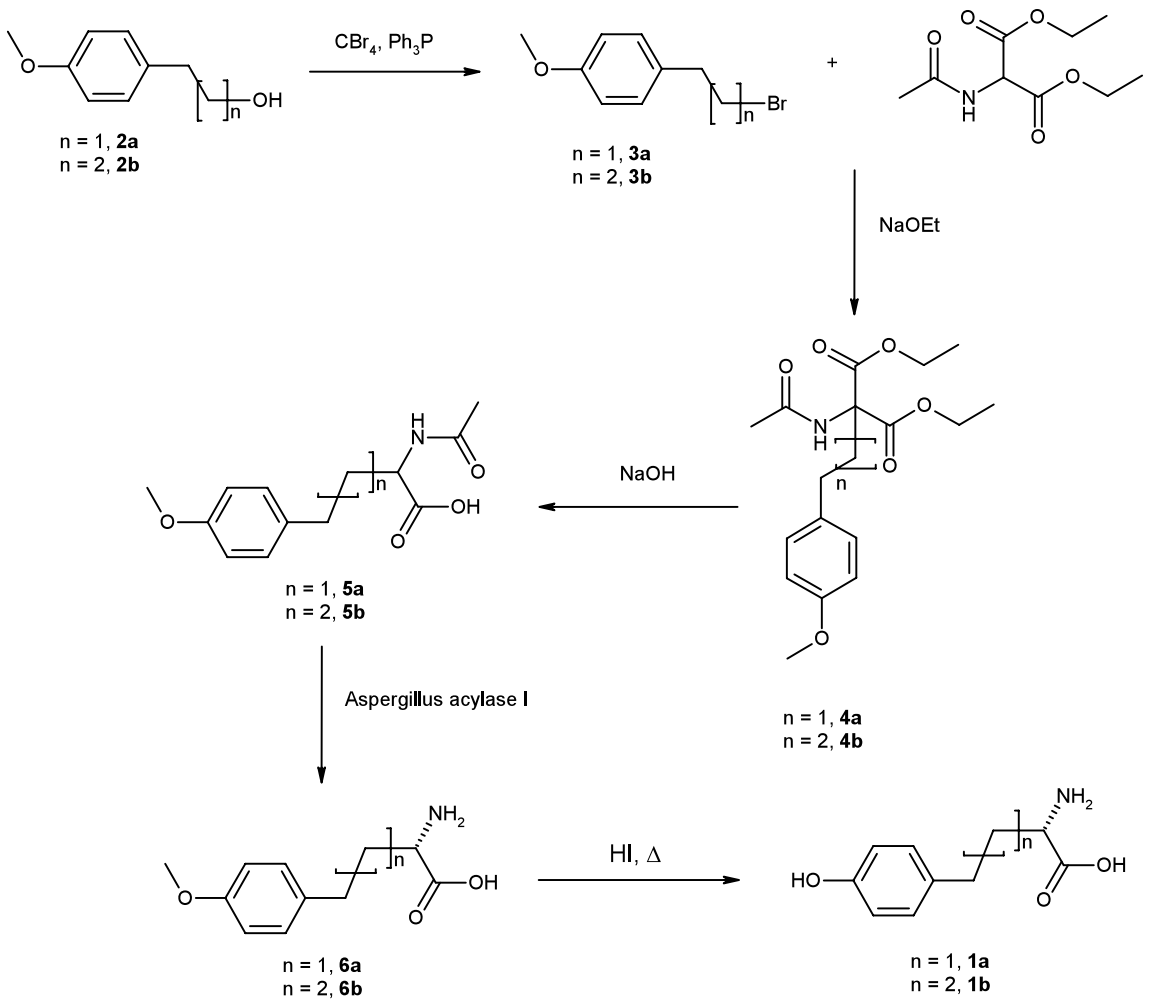

Scheme 2 Synthesis of tyrosine homologues and *O*-methyl derivatives

and analyzed by GlobalWorks software supplied by OLIS (Matheson 1990).

Results and discussion

Synthesis of tyrosine homologues and derivatives: The synthesis and enzymatic resolution of **6b** and **1b** (Shimohigashi et al. 1976; Ueno et al. 1975), and the asymmetric synthesis of **6a** (Yamada et al. 1998) and **1a** (Murashige et al. 2011) have been previously reported. In our hands, the most convenient method to obtain the optically active Tyr homologues and their *O*-methyl derivatives was by following a modified method of Shimohigashi et al. (1976), using diethyl acetamidomalonate, as described previously (Scheme 2) (Do et al. 2014). 2-(4-Methoxyphenyl)ethanol (**2a**) and 3-(4-methoxyphenyl)propanol (**2b**) are commercially available and were selected as starting materials. As Appel's salt is a milder reagent suitable for primary alcohols, when bromination was carried out using this reagent, we obtained excellent yield of **3**. Alkylation of **3** using diethyl acetamidomalonate in sodium ethoxide proceeded to give **4** in modest yield. Subsequent hydrolysis and decarboxylation of **4** was achieved in one step with excellent yield of the N-acetyl derivatives, **5a** and **5b,** by refluxing with two equivalents of NaOH in aqueous THF. Enantioselective hydrolysis of **5** using Aspergillus acylase (Chenault et al. 1989) was best carried out in phosphate buffer at pH 8 instead of water, due to the low solubility

Table 1 K_i values for tyrosine homologues

Inhibitors	K_i (mM)
L-Homotyrosine (**1a**)	0.80 mM ± 0.20
L-Bishomotyrosine (**1b**)	1.50 mM ± 0.50
O-Methoxy-L-homotyrosine (**6a**)	0.80 mM ± 0.17
O-Methoxy-L-bishomotyrosine (**6b**)	1.04 mM ± 0.18

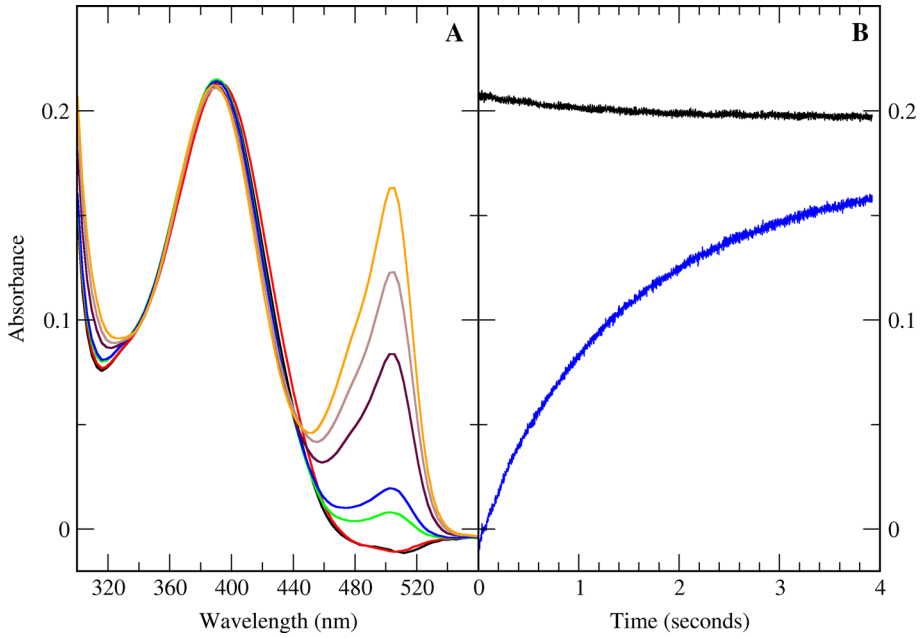

Fig. 2 Spectra and time course for reaction of TPL with 5 mM L-homotyrosine (**1a**). **a** Spectra at various times after mixing. **b** Time courses at 500 nm (*blue*) and 420 nm (*black*) (color figure online)

Table 2 Rate constants and absorption maxima of intermediate formation of homotyrosines with TPL

Compound	$1/\tau_1$	$1/\tau_2$	E_{AL} λ_{max} (nm)	E_Q λ_{max} (nm)
1a	3.0 ± 0.4	$(6.2 \pm 0.5) \times 10^{-1}$	387	505
1b	5.0 ± 0.3	2.39 ± 0.21	390	496
6a	5.3 ± 0.3	$(1.40 \pm 0.16) \times 10^{-1}$	394	499
6b	0.66 ± 0.01	0.14 ± 0.01	387	496

of compound **5** in water. Enzymatic resolution following this method proceeded to give the optically active **6a** and **6b** in good yield. To the best of our knowledge, this is the first report of the resolution of tyrosine homologues using acylase. *O*-Dealkylation of **6a** was previously reported to proceed in concentrated HCl, by refluxing for three days with optical activity remaining unaffected (Yamada et al. 1998). However, when this step was carried out in concentrated HI, we recovered similar yields for compound **1a** and **1b** within 15 h of reflux.

Enzyme inhibition: Our results indicated that compounds **1a**, **1b**, **6a**, and **6b** are competitive inhibitors of *C. freundii* TPL that exhibit K_i values in the range of 0.8–1.5 mM (Table 1), similar to that of L-phenylalanine (2 mM). It is interesting to note that compounds **1a** and **6a**, homologues with extension by one methylene unit, displayed slightly better inhibition than that of **1b** and **6b**, which were extended by two methylene units. Competitive inhibitors of TPL, L-alanine and L-methionine, form quinonoid complexes (Phillips et al. 2002; Milić et al. 2008). While L-alanine forms quinonoid complexes in both open and closed conformations, L-methionine forms a quinonoid structure only in the closed conformation (Milić et al. 2008). It was previously suggested that the phenolic OH of the substrate is hydrogen bonded to Arg381 at the active site (Sundararaju et al. 1997), which was later shown by the crystal structure of Y71F and F448H mutant TPL with 3-F-L-tyrosine bound (Milić et al. 2011). We were curious as to whether *O*-methylation would affect the inhibitory efficiency of the homologues. Our results in Table 1 show no difference between homologues **1a** and **1b** with their *O*-methyl derivatives **6a** and **6b**, suggesting that hydrogen bonding of the OH is not essential for binding of the inhibitors evaluated in this work. This also suggests that these homotyrosines do not form closed conformations on binding to TPL, since the hydrogen bonds to the OH are formed in the closed conformation. Previously, we reported the evaluation of 2- and 3-aza-L-tyrosines as inhibitors for TPL, with K_i values of 135 μM and 3.4 mM, respectively (Watkins and Phillips, 2001). Since 2-azatyrosine will exist as the phenolate ion at neutral pH, we suggested that this is consistent with binding of tyrosine to TPL as the phenolate. In comparison, the rationale behind our present design was to mimic the elongated structure of the keto-quinonoid transition state. However, the binding affinity of these compounds for TPL is not as high as 2-aza-L-tyrosine, but better than 3-aza-L-tyrosine.

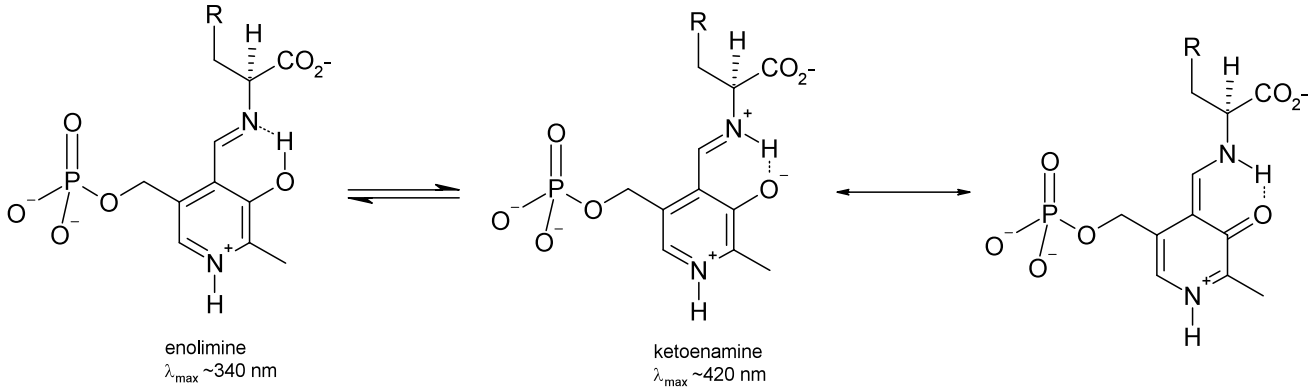

Scheme 3 PLP aldimine structures

Pre-steady-state kinetics: The absorbance spectra from the rapid-scanning stopped-flow experiments share many similarities between all compounds tested (Fig. 2 and Supplemental Data). The reaction of tyrosine with TPL was previously reported to give rise to two characteristic absorption maxima at $\lambda_{max} = 418$ and 502 nm, corresponding to the formation of external aldimine and quinonoid intermediates, respectively (Muro et al. 1978; Phillips et al. 2006). From our results, the presence of external aldimines was observed in all cases, indicated by unusually blue-shifted absorption maxima around $\lambda_{max} = 390$ nm (Fig. 2; Table 2). Also, the formation of quinonoid intermediates was also observed for all compounds, evident by normal quinonoid absorption maxima around $\lambda_{max} = 500$ nm. Surprisingly, the amplitude of the absorbance peak at 500 nm for *O*-methyl-L-homotyrosine (**6a**) is much smaller than L-homotyrosine (**1a**) and the bishomotyrosines (**1b** and **6b**) (Supplemental Data, Figure S1), even though there is little difference in the values of K_i. These data demonstrate that these inhibitors were bound to PLP at the active site leading to formation of an equilibrating mixture of external aldimine and quinonoid complexes. However, the low equilibrium concentration of the quinonoid complexes implies that they do not contribute significantly to the K_i values.

The absorption maxima of the aldimine intermediates for these tyrosine homologues are blue-shifted slightly from that reported (Muro et al. 1978; Phillips et al. 2006) in comparison with tyrosine as the substrate (Fig. 2). The strain that exists in aldimines in the aminotransferase family is well documented (Hayashi et al. 2003). Normally, the external aldimine bonds are in plane with the PLP, with a hydrogen bond formed between the iminium NH and the 3′-phenolate of the PLP (Scheme 3), and they exhibit absorption maxima at about 425 nm. This was observed with TPL reacting with other substrate analogues, such as L-methionine and L-alanine (Chen et al. 1995a,b; Phillips et al. 2002). The aldimine can also be drawn as the ketoenamine resonance structure (Scheme 3). However, if the imine is twisted out of the plane of the pyridine ring, the intramolecular hydrogen bonding is weakened, as well as the resonance between the iminium and the phenolate, resulting in the blue-shift in the absorbance maximum. In some cases, an equilibrium of the ketoenamine with an enolimine tautomer is present (Scheme 3), but this is not seen in TPL. Our results suggest that binding of the extended side chain of the tyrosine homologues results in strained aldimines with the iminium bond rotated out of plane of the PLP. This may be the result of steric restraints imposed by the extended side chains of these homologues. The energetic penalty resulting from the strain may be a reason for the weaker than expected binding of these homologues. However, the relatively normal absorption spectra and rates of formation of the quinonoid complexes suggest that they are not strained, possibly due to conformational changes of the enzyme upon quinonoid intermediate formation that relieve the strain. We note that the structure of F448H mutant TPL complexed with 3-fluorotyrosine demonstrates formation of a closed active site with a "tense" conformation of the quinonoid intermediate (Milić et al. 2011).

Conclusion

With promising results from our previous work on mechanism-based inhibitors of TIL, we extended our design and rationale to TPL, since both enzymes share remarkably similar mechanistic details in the cleavage of their physiological substrates. Also, it was also suggested that the hydrogen bond from the phenol of the substrate with Arg381 has an essential role in contributing to the C_α–C_β–C_γ bond angle strain that assisted in cleavage of the C_β–C_γ bond of the substrate. Based on the postulated mechanism of TPL, we explored the effect of homologation of the C_α position and deletion of the hydrogen bond donor site of phenol from the physiological substrate, in the search for mechanism-based inhibitors of TPL. Our results indicated

that the inhibition constant, K_i, of all inhibitors reported herein were in the range of 0.8–1.5 mM. Furthermore, pre-steady-state kinetic evaluations confirmed binding of these compounds at the active sites, forming an equilibrium mixture of aldimines and quinonoid intermediates. These results suggest that there may be conformational differences between TPL and TIL during catalysis.

Acknowledgments Financial support to Q. D. during his PhD work was provided by the University of Georgia.

Compliance with ethical standards

Conflict of interest The authors declare that they have no conflict of interest.

Research involving human participants and/or animals This article does not contain any studies with human participants or animals performed by any of the authors.

References

Antson AA, Demidkina TV, Gollnick P, Dauter Z, Von Tersch RL, Long J, Berezhnoy SN, Phillips RS, Harutyunyan EH, Wilson KS (1993) Three-dimensional structure of tyrosine phenol-lyase. Biochemistry 32:4195–4206

Chen HY, Demidkina TV, Phillips RS (1995a) Site-directed mutagenesis of tyrosine-71 to phenylalanine in *Citrobacter freundii* tyrosine phenol-lyase: evidence for dual roles of tyrosine-71 as a general acid catalyst in the reaction mechanism and in cofactor binding. Biochemistry 34:12276–12283

Chen H, Gollnick P, Phillips RS (1995b) Site-directed mutagenesis of His343-Ala in *Citrobacter freundii* tyrosine phenol-lyase. Effects on the kinetic mechanism and rate-determining step. Eur J Biochem 229:540–549

Chenault HK, Dahmer J, Whitesides GM (1989) Kinetic resolution of unnatural and rarely occurring amino acids: enantioselective hydrolysis of N-acyl amino acids catalyzed by acylase I. J Am Chem Soc 111:6354–6364

Cleland WW (1979) Statistical analysis of enzyme kinetic data. Meth Enzymol 63:103–138

Di Martino P, Merieau A, Phillips R, Orange N, Hulen C (2002) Isolation of an *Escherichia coli* strain mutant unable to form biofilm on polystyrene and to adhere to human pneumocyte cells: involvement of tryptophanase. Can J Microbiol 48:132–137

Do QT, Nguyen GT, Celis V, Phillips RS (2014) Inhibition of *escherichia coli* tryptophan indole-lyase by homologues of tryptophan. Arch Biochem Biophys 560:20–26

Hayashi H, Mizuguchi H, Miyahara I, Islam MM, Ikushiro H, Nakajima Y, Hirotsu K, Kagamiyama H (2003) Strain and catalysis in aspartate aminotransferase. Biochim Biophys Acta 1647:103–109

Isupov MN, Antson AA, Dodson EJ, Dodson GG, Dementieva IS, Zakomirdina LN, Wilson KS, Dauter Z, Lebedev AA, Harutyunyan EH (1998) Crystal structure of tryptophanase. J Mol Biol 276:603–623

Kumagai H, Matsui H, Ohgishi K, Ogata K, Yamada H, Ueno T, Fukami H (1969) Synthesis of 3,4-dihydroxyphenyl-L-alanine from L-tyrosine and pyrocatechol by crystalline β-tyrosinase. Biochem Biophys Res Comm 34:266–270

Kumagai H, Yamada H, Matsui H, Ohgishi H, Ogata K (1970a) Tyrosine phenol lyase. I. Purification, crystallization, and properties. J Biol Chem 245:1767–1772

Kumagai H, Yamada H, Matsui H, Ohgishi H, Ogata K (1970b) Tyrosine phenol lyase. II. Cofactor requirements. J Biol Chem 245:1773–1777

Matheson IBC (1990) A critical comparison of least absolute deviation fitting (robust) and least-squares fitting: the importance of error distributions. Comput Chem 14:49–57

Milić D, Demidkina TV, Faleev NG, Matkovic-Calogovic D, Antson AA (2008) Insights into the catalytic mechanism of tyrosine phenol-lyase from X-ray structures of quinonoid intermediates. J Biol Chem 283:29206–29214

Milić D, Demidkina TV, Faleev NG, Phillips RS, Matkovic-Calogovic D, Antson AA (2011) Crystallographic snapshots of tyrosine phenol-lyase show that substrate strain plays a role in C-C bond cleavage. J Am Chem Soc 133:16468–16476

Murashige R, Hayashi Y, Ohmori S, Torii A, Aizu Y, Muto Y, Murai Y, Oda Y, Hashimoto M (2011) Comparisons of *O*-acylation and Friedel-Crafts acylation of phenols and acyl chlorides and Fries rearrangement of phenyl esters in trifluoromethanesulfonic acid: effective synthesis of optically active homotyrosines. Tetrahedron 67:641–649

Muro T, Nakatani H, Hiromi K, Kumagai H, Yamada H (1978) Elementary processes in the interaction of tyrosine phenol-lyase with inhibitors and substrate. J Biochem (Tokyo) 84:633–640

Phillips RS (1987) Reactions of *O*-acyl-L-serines with tryptophanase, tyrosine phenol-lyase, and tryptophan synthase. Arch Biochem Biophys 256:302–310

Phillips RS (1991) Reaction of indole and analogues with amino acid complexes of *Escherichia coli* tryptophan indole-lyase: detection of a new reaction intermediate by rapid-scanning stopped-flow spectrophotometry. Biochemistry 30:5927–5934

Phillips RS (2000) Proton transfer and carbon-carbon bond cleavage in the elimination of indole catalyzed by *Escherichia coli* tryptophan indole-lyase. J Am Chem Soc 122:1008–1014

Phillips RS, Ravichandran K, Tersch RV (1989) Synthesis of L-tyrosine from phenol and S-(*o*-nitrophenyl)-L-cysteine catalyzed by tyrosine phenol-lyase. Enz Microb Technol 11:80–83

Phillips RS, Demidkina TV, Zakomirdina LN, Bruno S, Ronda L, Mozzarelli A (2002) Crystals of tryptophan indole-lyase and tyrosine phenol-lyase form stable quinonoid complexes. J Biol Chem 277:21592–21597

Phillips RS, Chen HY, Faleev NG (2006) Aminoacrylate intermediates in the reaction of *Citrobacter freundii* tyrosine phenol-lyase. Biochemistry 45:9575–9583

Shimohigashi Y, Lee S, Izumiya N (1976) Resolution of amino acids. XII. Preparation of L-2-amino-5-arylpentanoic acids, constituent amino acids in AM-toxins. Bull Chem Soc Jpn 49:3280–3284

Snell EE (1975) Tryptophanase: structure, catalytic activities, and mechanism of action. Adv Enzymol Relat Areas Mol Biol 42:287–333

Sundararaju B, Antson AA, Phillips RS, Demidkina TV, Barbolina MV, Gollnick P, Dodson GG, Wilson KS (1997) The crystal structure of C*itrobacter freundii* tyrosine phenol-lyase complexed with 3-(4′-hydroxyphenyl)propionic acid, together with site-directed mutagenesis and kinetic analysis, demonstrates that arginine-381 is required for substrate specificity. Biochemistry 36:6502–6510

Ueno T, Nakashima T, Hayashi Y, Fukami H (1975) Structures of AM-toxin I and II, host specific phytotoxic metabolites produced by *Alternaria mali*. Agri Biol Chem 39:1115–1122

Venkatesh M, Mukherjee S, Wang H, Li H, Sun K, Benechet AP, Qiu Z, Maher L, Redinbo MR, Phillips RS, Fleet JC, Kortagere S,

Mukherjee P, Fasano A, Le Ven J, Nicholson JK, Dumas ME, Khanna KM, Mani S (2014) Symbiotic bacterial metabolites regulate gastrointestinal barrier function via the xenobiotic sensor PXR and toll-like receptor 4. Immunity 41:296–310

Watanabe T, Snell EE (1972) Reversibility of the tryptophanase reaction: synthesis of tryptophan from indole, pyruvate, and ammonia. Proc Nat Acad Sci USA 69:1086–1090

Watkins EB, Phillips RS (2001) Enzymatic synthesis of aza-L-tyrosines. Bioorg Med Chem Lett 11:2099–2100

Yamada H, Kumagai H, Matsui H, Ohgishi H, Ogata K (1968) Crystallization and properties of β-tyrosinase from *Escherichia intermedia*. Biochem Biophys Res Comm 33:10–14

Yamada M, Nagashima N, Hasegawa J, Takahashi S (1998) A highly efficient asymmetric synthesis of methoxyhomophenylalanine using Michael addition of phenethylamine. Tet. Lett. 39:9019–9022